

## SOME ASSOCIATION PROPERTIES OF BOVINE SH- $\kappa$ -CASEIN

H.J. VREEMAN, J.A. BRINKHUIS and C.A. VAN DER SPEK

*Netherlands Institute for Dairy Research (NIZO), P.O. Box 20, 6710 BA Ede, The Netherlands*

Received 1 April 1981

Revised manuscript received 4 August 1981

(1) It is shown that  $\kappa$ -casein association is characterized by a critical micelle concentration which decreases as the ionic strength is increased. (2) The  $\kappa$ -casein polymer molecular weight was calculated from the weight-average apparent molecular weight by taking into consideration the monomer concentration and the excluded volume. The degree of polymerization is 30 and does not depend on ionic strength between 0.1 and 1 M. (3) The non-electrical contribution to the standard free energy of association is  $-38$  kJ/mol monomer. The electrical part is small: 1–2 kJ/mol monomer depending on the ionic strength and  $\kappa$ -casein genetic variant. (4) The limitation of size and the size itself of the  $\kappa$ -casein polymer can be explained by the theory of self-assembly of virus particles by Caspar and Klug (D.L.D. Caspar and A. Klug, Cold Spring Harb. Symp. Quant. Biol. 27 (1962)1). (5) Extending this theory to casein micelle assembly, it is predicted that micelles are distributed preferentially over a restricted number of sizes.

### 1. Introduction

Nearly 80% of the protein in bovine skim milk is a stable suspension of large colloidal aggregates called casein micelles. About 12.5% of the casein is  $\kappa$ -casein and this fraction acts as a protective colloid to prevent precipitation of the other calcium-sensitive caseins [1,2]. The properties of  $\kappa$ -casein are important for the stabilization of the micelle suspension as is illustrated by the action of the enzyme chymosin (EC 3.4.23.4) on milk, whereby a single peptide bond in  $\kappa$ -casein is rapidly split which causes flocculation of the micelles. It is known that  $\kappa$ -casein itself is soluble in calcium-containing media and shows a monomer-high-polymer association behaviour [2,3]. As judged from sedimentation in the analytical ultracentrifuge the  $\kappa$ -casein polymer distribution is narrow. The polymer has a temperature-insensitive sedimentation rate of about 13 S [3]. The purpose of this communication is to describe the molecular weight determination of this polymer and to advance a theory for casein micelle formation.

### 2. Materials and methods

The experiments were made with SH- $\kappa$ -casein A<sub>1</sub> (0.60) or B<sub>1</sub> (0.52) (for nomenclature see ref. [3]) dissolved in buffers containing 0.01 M EDTA and either 0.001 M dithiothreitol or 0.003 M mercaptoethanol and 0.1, 0.2, 0.5 and 1 M NaCl, respectively, at pH 7.0. The  $\kappa$ -casein was prepared as described previously [3]. To obtain reproducible results it appeared necessary to depolymerize the protein in 6 M guanidine-HCl + dithiothreitol for about 1 week prior to dialysis against the buffers.

Density measurements were carried out in an Anton Paar (Graz, Austria) DMA-02C densitometer [4].

Viscosities were measured with two Ubbelohde viscometers with 240 and 330 s flow time for water (20°C), respectively.

Sedimentation experiments were carried out in a Spinco E analytical ultracentrifuge using a 12 mm single-sector carbon-filled Epon centrepiece for sedimentation velocity experiments and a 12 mm double-sector A1-filled Epon centrepiece for

the Trautman procedure. The sedimentation rates were determined at 20–22°C; the sedimentation coefficients were corrected to standard conditions (20°C, water) by the usual corrections: (a) a density correction from density measurements made for the determination of the density increment extrapolated to zero concentration  $(\delta\rho/\delta c)_0$ ; (b) the viscosity correction from measurements made for the determination of the intrinsic viscosity.

Calculations were performed on an HP 9830 A calculator; surface areas under schlieren curves on 10× enlarged prints from schlieren photographs were determined with the HP 9864 A digitizer.

### 2.1. Molecular weight determination

Apparent weight-average molecular weights were determined as a function of the protein concentration by the method of Trautman [5]. The basic equation is:

$$M_{w,app} = RT(dc/dr)_m / \{ (\delta\rho/\delta c)_0 \omega^2 r_m c_m \} \quad (1)$$

where  $R$  is the gas constant,  $T$  the absolute temperature,  $\omega$  the angular velocity,  $r_m$  the distance of the meniscus from the centre of rotation,  $(\delta\rho/\delta c)_0$  the density increment,  $c_m$  and  $(dc/dr)_m$  the concentration and concentration gradient at the meniscus. In the Trautman plot  $(dc/dr)_m/\omega^2$  is plotted against  $\Delta c$  where  $\Delta c = c_0 - c_m$  and  $c_0$  is the initial protein concentration. In practice, we used  $\Delta c = (c_0 - c_p) + (c_p - c_m)$ , where  $c_p$  is the concentration in the plateau region,  $c_0 - c_p = \{1 - \exp(-2\omega^2 s t)\} c_0$  and  $(c_p - c_m)$  is proportional to the surface area under the schlieren curve between the meniscus and plateau region. For this procedure,  $c_0$  and  $s$  must be determined in separate experiments but the eventual result is more accurate than evaluating  $c$  from the Kleiner and Kegeles integral:

$$c_0 - c_m = (1/r_m^2) \int_{r_m}^{r_p} r^2 (\delta c/\delta r) dr \quad (2)$$

It appears that the Trautman plot is well suited to determine the critical micelle concentration (CMC) of the monomer-single-polymer type of self-association that was studied here. This can be seen

easily if eq. (1) is rewritten for the ideal case:

$$RT(dc/dr)_m / (\delta\rho/\delta c)_0 \omega^2 r_m = M_w \cdot c = M_1 c_1 + M_n c_n \quad (3)$$

where  $c_1$ ,  $c_n$  and  $c$  are the monomer, polymer and total concentration, respectively, at the meniscus,  $n$  the degree of polymerization in  $nM_1 = M_n$ ;  $c_n = 0$  for  $c < \text{CMC}$  and  $c_1 = \text{CMC}$  for  $c > \text{CMC}$ .

### 2.2. Determination of the degree of polymerization and 2nd virial coefficient

$M_{w,app}$  differs from the weight-average molecular weight ( $M_w$ ) by a non-ideality term as follows [6a,7a]

$$M_{w,app} = M_w - 2A_2 c \quad (4)$$

where the second virial coefficient

$$A_2 = \sum_i \sum_j M_i M_j A_{ij} w_i w_j \quad (5)$$

and

$$w_i = c_i / c \quad (6)$$

The coefficients  $A_{ij}$  for spherical particles are given by (cf. ref. [7b])

$$A_{ij} = (N_a / 2 M_i M_j) \int_0^\infty (1 - \exp(-V_{ij}/kT)) \times 4\pi r_{ij}^2 dr_{ij} \quad (7)$$

where  $N_a$  is Avogadro's number,  $V_{ij}$  the intermolecular potential between particles  $i$  and  $j$  and  $r_{ij}$  the distance between the centres of the respective spheres. For a hard-sphere potential:  $V_{ij} = \infty$  for  $0 \leq r_{ij} \leq R_i + R_j$  and  $V_{ij} = 0$  for  $r_{ij} > R_i + R_j$  ( $R$  = sphere radius) and in that case:

$$A_{ij} = \frac{2\pi N_a}{3 M_i M_j} (R_i + R_j)^3 \quad (8)$$

With this result eq. (4) becomes

$$M_{w,app} = M_w - \frac{4\pi N_a}{3} c \sum_i \sum_j (R_i + R_j)^3 w_i w_j \quad (9)$$

For a single species this equation reduces to

$$M_{app} = M(1 - 8vc) \quad (10)$$

where  $v$  is the specific volume of the particle. The more familiar reciprocal relation which can be obtained from eq. (10) is (dropping terms containing  $c^2$  and higher):

$$1/M_{\text{app}} = 1/M + Bc \quad (11)$$

where  $B = 8v/M$ . When self-association of the protein occurs it is convenient and reasonable to suppose that its specific volume will remain constant. In that case, for a monomer-single-polymer equilibrium, using eq. (9), eq. (4) can be rewritten as

$$M_{\text{w,app}} = M_w(1 - fvc) \quad (12)$$

$$\text{where } f = \left( 8w_1^2 + 2(1 + n^{1/3})^3 w_1 w_2 + 8w_2^2 n \right) / (w_1 + w_2 n) \quad (13)$$

In fig. 1,  $f$  is given as a function of composition and increasing degree of association. Remembering that the viral term is after all a correction term, which one does not need to know too accurately, it appears that for small  $n$  the factor  $f \approx 8$  and the 'single species' eq. (1) or eq. (11) can be used. In our case,  $n$  is high so that  $f$  had to be calculated for each concentration. From sedimentation velocity experiments (cf. fig. 2) and equilibrium experiments (cf. fig. 4) it follows that the polymer particle has little tendency to increase its size above a concentration of about 3 g/l. Therefore, it is assumed that  $n$  is independent of the total protein concentration. As the monomer concentration remains approximately constant for total concentrations larger than the critical micelle concentration,  $M_{\text{w,app}}$  (calc.) is a function of  $n$ ,  $v$  and  $c$  only (cf. eq. (12)). In a least-squares grid-

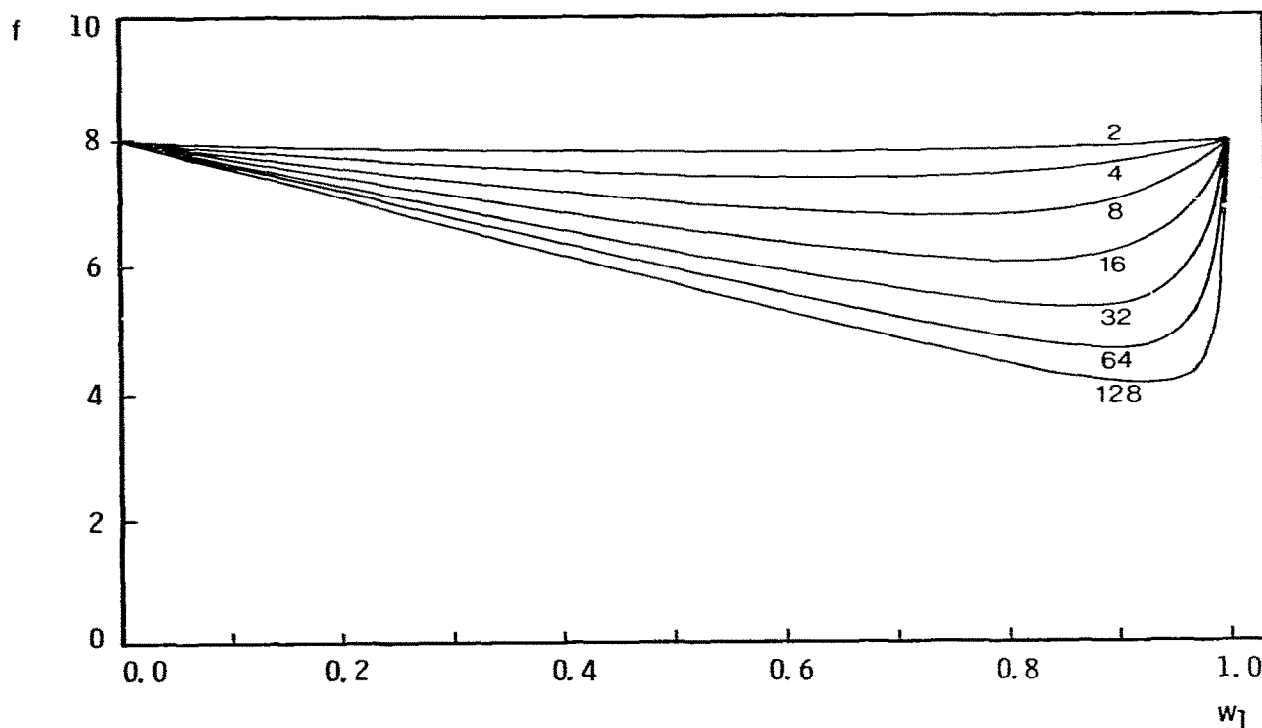


Fig. 1. The second virial factor  $f$  for a solution containing a mixture of monomers and polymers (cf. eq. (13)) as a function of the weight fraction of monomer  $w_1$ . The numbers given with the curves refer to the degree of polymerization of the polymer.

search program the values for  $n$  and  $v$  were found which gave the best fit of  $M_{w,app}$  (calc.) to  $M_{w,app}$  (expt.) [8]. Only that part of the  $M_{w,app}$  versus  $c$  curve well above the CMC was used in the grid-search. This has two reasons: (a) the factor  $f$  changes rapidly in the neighbourhood of the CMC (cf. fig. 1) so that a small error in the CMC has a pronounced effect on  $f$ , and (b) the assumption that the monomer concentration is constant for  $c > \text{CMC}$  is in conflict with the fact that  $A_2$  (cf. eq. (4)) is non-zero, i.e., the activity coefficient varies with the concentration. The error introduced in  $M_{w,app}$  (calc.) by a non-constant  $c_1$  is largest when the term  $c_1 M_1$  dominates, i.e., near the CMC.

### 3. Results

#### 3.1. Sedimentation coefficients

In fig. 2 the sedimentation coefficients reduced to standard conditions are plotted against the polymer concentration, i.e., total concentration minus CMC; the extrapolated values to zero polymer concentration,  $s_{20,w}^0$ , are given in table 1. The ratio  $K_s/[\eta]$  depends on the form of the particle ( $K_s$  from  $1/s = (1/s_0)(1 + K_s c)$  [9]). Therefore this ratio is also given in table 1.

#### 3.2. Molecular weight

A typical example of a Trautman plot for SH- $\kappa$ -casein is shown in fig. 3. The least-squares second-degree curve through the experimental points bends

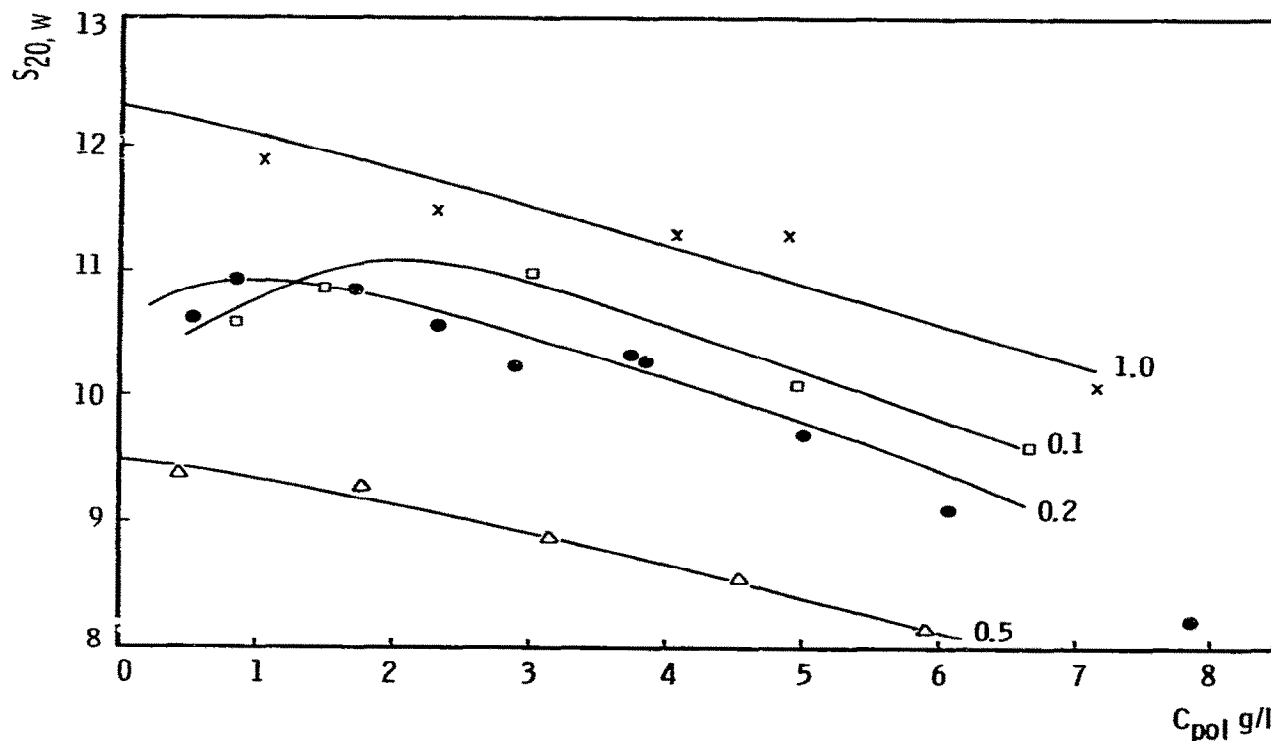


Fig. 2. Sedimentation rates of SH- $\kappa$ -casein in 0.01 M EDTA, 0.001 M dithiothreitol plus NaCl, at pH 7.0 as a function of the polymer concentration:  $\square$ , 0.1 M NaCl;  $\bullet$ , 0.2 M NaCl;  $\triangle$ , 0.5 M NaCl;  $\times$ , 1 M NaCl.

Table 1

Hydrodynamic parameters of SH- $\kappa$ -casein at varying ionic strength

Buffer (M NaCl)	$(\delta\rho/\delta c)_0$	$\rho_0$ (g/ml)	$\eta_0$ (mPa·s)	$[\eta]$ (ml/g)	$s_{20,w}^0$ (S)	$K_s/[\eta]$
0.1	0.2574	1.0046	1.020	15.6	12.0	2.1
0.2	0.2544	1.0086	1.029	15.9	11.6	1.8
0.5	0.2453	1.0206	1.058	16.7	9.5	1.7
1.0	0.2301	1.0408	1.106	15.7	12.3	1.5

slightly towards the  $\Delta c$ -axis for small  $\Delta c$  (i.e., large  $c_m$ ). This is because the non-ideality term becomes increasingly important as the concentration increases [6c]. On the  $\Delta c$ -axis, the initial concentration  $c_0$ , determined in a separate synthetic-boundary experiment, is indicated. The broken line represents the hypothetical Trautman plot for

monomer  $\kappa$ -casein accepting a monomer molecular weight of 19030. It intersects the 'polymer' line left of  $c_0$ ; the difference between  $c_0$  and the abscissa of the point of intersection is the CMC. The least-squares polynomial obtained in the Trautman plot is used to construct the solid line in the  $M_{w,app}$  versus  $c$  plot according to eq. (1) (cf. fig. 4). It

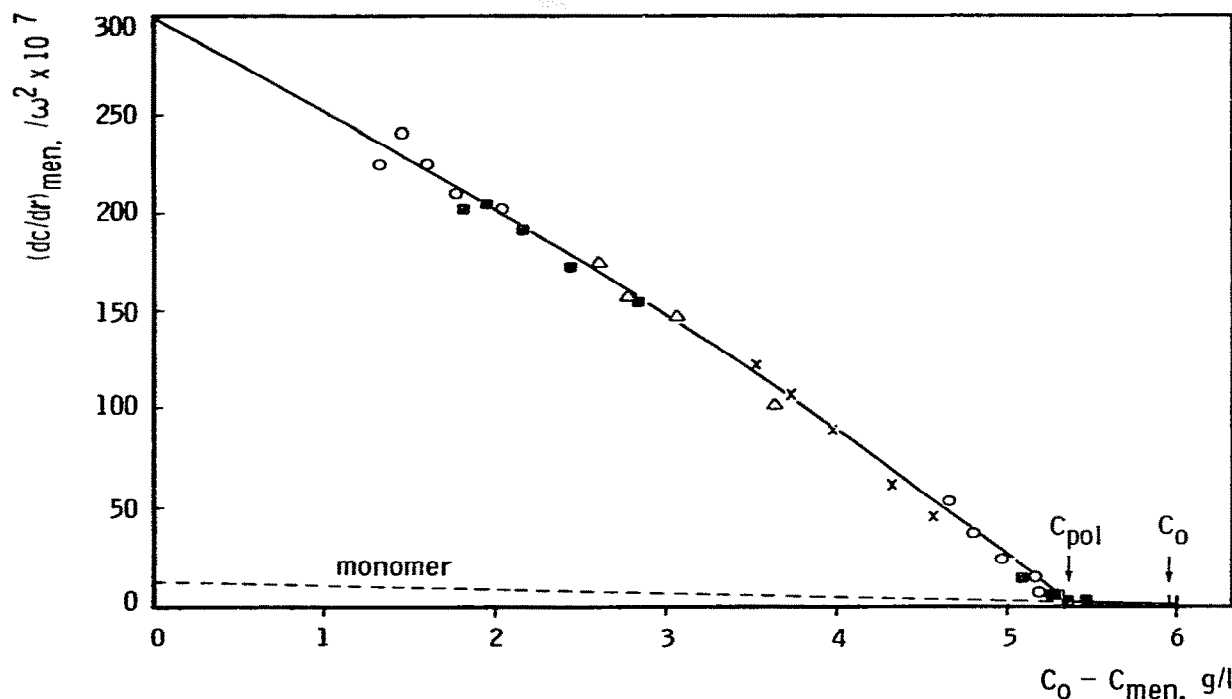


Fig. 3. Trautman plot for SH- $\kappa$ -casein in buffer containing 0.1 M NaCl. From left to right the rotor speeds are (in rpm):  $\circ$ , 4800;  $\blacksquare$ , 6000;  $\triangle$ , 7200;  $\times$ , 9000;  $\circ$ , 12000;  $\blacksquare$ , 15000. The  $(dc/dr)_{men}$  is expressed in mm on the print of the schlieren pattern. To calculate  $M_{w,app}$  the conversion factor including  $RT/\{(\delta\rho/\delta c)_0 r_m\}$  is  $8952 \times 10^7$ .

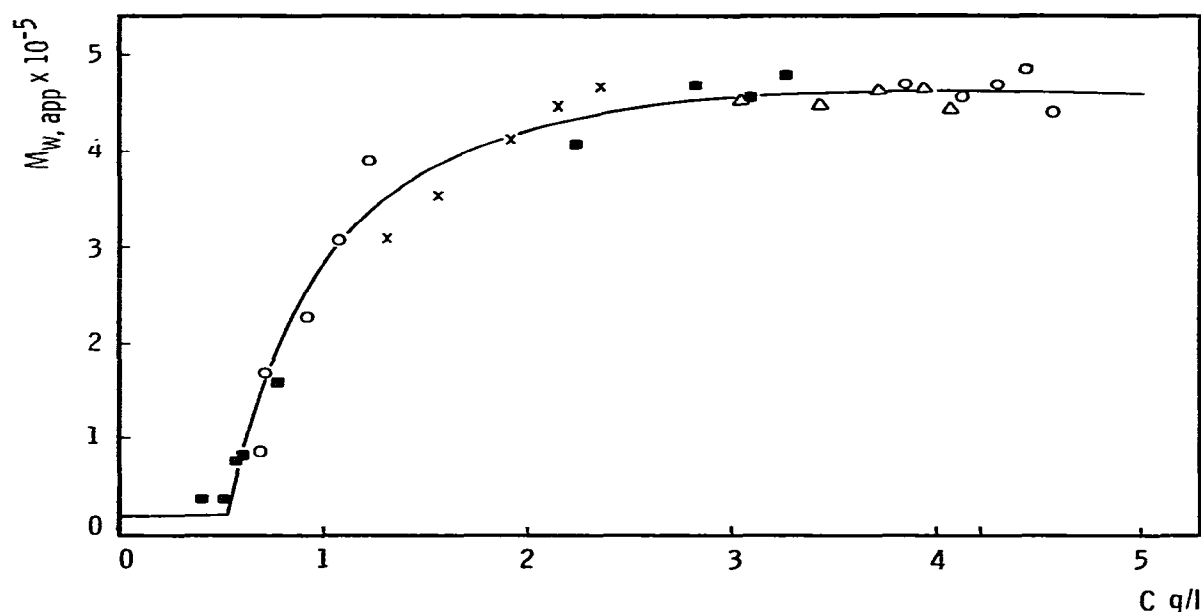


Fig. 4. Weight-average apparent molecular weight of SH- $\kappa$ -casein in buffer containing 0.1 M NaCl. For calculation of the line (according to eq. (1)) the  $(dc/dr)_{men}$  is taken from fig. 3 (solid line).

appeared easier to smooth the data in this way on the Trautman plot than on the  $M_{w,app}$  versus  $c$  plot. Using the smoothed data, the degree of polymerization  $n$  and the second virial coefficient (i.e., the specific volume  $v$ ) were determined from eq. (12), assuming that  $n$  and the monomer concentration  $c_1$  are constant over the whole concentration range. The relevant data are collected in table 2. The standard free energy of transfer of a mole of monomers from solution into polymers was calculated from  $\Delta G^0 = RT \ln(CMC)$  where the CMC is in mole-fraction units [3].

## 4. Discussion

### 4.1. Hydrodynamic measurements

The ratio  $K_s/[\eta]$  found for the polymer particle (cf. table 1) is consistent with a spherical shape of the particle. For spherical particles the ratio should be 1.66 [9] whereas in the case of more elongated particles much lower ratios are found, e.g., 0.62 for fibrinogen [9]. The high ratio of 2.1 in 0.1 M NaCl buffer has no theoretical explanation as yet but is not infrequently observed for other proteins [9].

Table 2

Association number, specific volume from the excluded volume, critical micelle concentration and standard free energy of association of SH- $\kappa$ -casein

Buffer (M NaCl)	$n$ (monomers/polymer)	$v$ (ml/g)	CMC (g/l)	$-\Delta G^0$ (kJ/mol per monomer)
0.1	31.4	3.7	0.53	35.4
0.2	29.5	4.3	0.51	35.4
0.5	29.5	2.4	0.42	35.9
1.0	34.9	5.3	0.24	37.4

For a spherical particle an effective hydrodynamic radius can be calculated from the extrapolated sedimentation coefficient and (independently) from the intrinsic viscosity as follows (cf. ref. [10])

$$R_s = M(\delta\rho/\delta c)_0 / (6\pi\eta_0 s_{20,w}^0 N_a) \quad (14)$$

$$R_\eta = \{(0.3M[\eta]) / (\pi N_a)\}^{1/3} \quad (15)$$

These radii are listed in table 3. No significant trend with increasing ionic strength is apparent. If the particles were elongated,  $R_s$  and  $R_\eta$  calculated from eqs. (14) and (15) would not be equal. It can be concluded from table 3 that the SH- $\kappa$ -casein polymer is a sphere with a diameter which is practically constant and equal to 23 nm between 0.1 and 1.0 M NaCl. The specific volume for this particle is 6.7 ml/g, which makes it much more voluminous than a globular protein which has a specific volume of about 1 ml/g [10], but not as much as a random coil which would give an  $[\eta]$  of 21 ml/g in this case [11]. Furthermore, for a random coil  $R_\eta/R_s = 1.3$  if the radii are again calculated by eqs. (14) and (15) [10]. Therefore, the hydrodynamic behaviour of the SH- $\kappa$ -casein polymer is not typical of that of a random coil.

#### 4.2. Molecular weight

The specific volume which was found from the excluded volume correction (cf. table 2) is of the same order as that which was calculated in the preceding section from  $[\eta]$  or  $S$ . The accuracy cannot be expected to be very high because  $A_2c$  is a correction term. The same values of  $n$  were found when  $A_2$  was calculated with a fixed value of  $v = 6.7$  ml/g, followed by a least-squares itera-

tion for  $n$ . It is concluded that there are about 30 monomers in an SH- $\kappa$ -casein polymer independent of the experimental conditions.

#### 4.3. Standard free energy of association

The ionic strength is of minor influence on the SH- $\kappa$ -casein polymer molecular weight. The electrical contribution to the free energy was calculated using [10b]:

$$W_{el} = (Ze)^2 / (2\epsilon R(1 + \kappa R)) \quad (16)$$

where  $Ze$  is the net charge,  $e$  the elementary charge,  $\epsilon$  the dielectric constant,  $R$  the radius of the particle and  $\kappa$  the Debye-Hückel parameter. This Debye-Hückel approximation can be used because the surface potential is low ( $\approx 10$  mV). The following model was applied: the species are spherical and the specific volumes of monomer and polymer are equal. The net charge of the monomer at pH 7.0 is  $-2.5$  for the genetic B-variant and  $-3.5$  for the A-variant of  $\kappa$ -casein, the radius of the polymer is 11.5 nm. The electrical free energy of addition of the last monomer to the polymer is  $W_{el,30} - W_{el,29} - W_{el,1}$ , where  $W_{el,n}$  is the  $W_{el}$  for the  $n$ -mer. The result is 2.4 kJ/mol monomer at 0.1 M NaCl decreasing to 0.7 kJ/mol monomer at 1 M NaCl for the A-variant, the result for the B-variant is half as much because it has a smaller charge. This decrease explains the change in CMC with ionic strength, although the data are not accurate enough to preclude a salting-out contribution. The non-electrical contribution to the free energy then is  $-38$  kJ/mol monomer. Clearly, the electrical repulsion is not sufficient by far to explain that the growth of the polymer stops at a limit of 30 monomers. Instead a steric constraint could well be the limiting factor.

#### 4.4. Model of the SH- $\kappa$ -casein polymer

If it is assumed that the SH- $\kappa$ -casein monomer has a conformation which is basically invariant and that therefore interaction with other monomers may occur via specific bonds, then it is possible to apply the principles which have been formulated for the self-assembly of virus particles [12]. It

Table 3

Equivalent sphere radii of the SH- $\kappa$ -casein polymer from sedimentation and viscosity

Buffer (M NaCl)	$R_s$ (nm)	$R_\eta$ (nm)
0.1	11.1	11.4
0.2	10.6	11.2
0.5	12.2	11.4
1.0	10.1	11.9

appears that there is not a large number of possibilities to arrange identical asymmetric units on a sphere in such a manner that each unit is surrounded by others in an equivalent (or semi-equivalent) way. In fact, there is only one arrangement which is most efficient and that is an assembly of 60 units in icosahedral symmetry. This principle of strict equivalence is also valid for an arrangement of 30 dimers (or 20 trimers, or 12 pentamers). Furthermore, if it is now assumed that the SH- $\kappa$ -casein monomer unit has a pseudo two-fold symmetry, its polymer would thus be an assembly of 30 monomers in icosahedral symmetry. An example of a shell of 30 dimers is the polymer of alfalfa mosaic virus protein [13]; this protein also shows monomer-polymer association.

The large specific volume of the SH- $\kappa$ -casein polymer could be explained by an arrangement of the protein around a hollow, water-filled centre. Alternatively, it may be assumed that only the para- $\kappa$ -casein part of  $\kappa$ -casein (i.e., the first 105 amino acid residues out of a total of 169) forms an icosahedral core and that the macropeptide part (i.e., the C-terminal 64 amino acids) is extended and has a more random nature. For a random polypeptide chain attached to a plane surface by one end, a rough estimate of the thickness is the mean square distance of the amino acid segments from the plane:  $\langle x^2 \rangle = 7/18 \, il^2$ ; where  $i$  is the number of segments and  $l$  the segment length [14]. For  $il^2$  the value found for an unattached polypeptide random coil may be taken. We used the expression given by Tanford [15] which relates the experimentally determined polypeptide chain dimensions to the chain length. The thickness of a layer of polypeptide chains of 64 amino acids is then 4.5 nm. In that case the para- $\kappa$ -casein core of the polymer has a radius of 7 nm and a specific volume of 2.3 ml/g.

#### 4.5. Casein micelles

If  $\kappa$ -casein has the properties of a virus coat-protein, then this must have consequences for the size of the casein micelles. The theory of Caspar and Klug [12] predicts that spherical shells consisting of  $60Pi^2$  monomers are favoured (the class  $P = 1, 3, 7, \dots$  and  $i$  is an integer). Most viruses are

found to belong to class  $P = 1$  [12]. The length of the nucleic acid chain will be a factor limiting the number of sizes to a specific one.

The function of  $\kappa$ -casein is to solubilize the other, insoluble caseins and no such restriction to one size is necessary. This means that the casein micelle distribution consists of a number of peaks. These correspond, e.g., for class  $P = 1$ , to micelles having 30, 120, 270, 480, etc.,  $\kappa$ -casein monomers.

From these numbers one can calculate that the radii of the casein micelles must be multiples of the radius of the  $\kappa$ -casein 30-mer. Micelles of class  $P > 1$  cannot be excluded a priori, so that the numbers 90, 210, 360, 390, etc., are additional possibilities. On electron micrographs it can be seen that casein micelles are indeed spherical [16]. For a property which depends on the radius as, for instance, the sedimentation velocity, this means that the resolution is highest in the small particle region. Some preliminary sedimentation experiments with uncooled and defatted milk from individual cows demonstrated the existence of a number of discrete peaks with sedimentation coefficients between 50 and 500 S and a large rapidly broadening peak containing the bulk of the material with higher sedimentation rates. Each milk proved its individuality by showing a selection of up to three peaks from a total of six found in all. Most of the casein micelle distributions have been obtained by electron-microscopy. But apart from an abrupt cut-off at the small micelle side the volume distributions are smooth with only one maximum [17], except in the study of Holt et al. [18] who find two maxima. With the sectioning techniques which were predominantly used, however, it is not immediately obvious from the photographs whether discrete micelle sizes exist.

#### References

- [1] K. Linderstrøm-Lang, C.R. Trav. Lab. Carlsberg 17 (1929) 1.
- [2] D.F. Waugh and P.H. von Hippel, J. Am. Chem. Soc. 78 (1956) 4576.
- [3] H.J. Vreeman, P. Both, J.A. Brinkhuis and C.A. van der Spek, Biochim. Biophys. Acta 491 (1977) 93.
- [4] G. Guérin, H.J. Vreeman and T.C. Nguyen, Eur. J. Biochem. 67 (1976) 433.



- [5] R. Trautman, J. Phys. Chem. 60 (1956) 1211.
- [6] H. Fujita, Foundations of ultracentrifugal analysis (J. Wiley, New York, 1975); a. pp. 207–212; b. 379–380; c. 213–214.
- [7] H. Yamakawa, Modern theory of polymer solutions (Harper and Row, New York, 1971); a. pp. 193–302; b. p. 182.
- [8] P.R. Bevington, Data reduction and error analysis for the physical sciences (McGraw-Hill, New York, 1969) pp. 204–246.
- [9] J.M. Creeth and C.G. Knight, Biochim. Biophys. Acta 102 (1965) 549.
- [10] C. Tanford, Physical chemistry of macromolecules (J. Wiley, New York, 1961); a. pp. 346–412; b. p. 465.
- [11] C. Tanford, K. Kawahara and S. Lapanje, J. Am. Chem. Soc. 89 (1967) 729.
- [12] D.L.D. Caspar and A. Klug, Cold Spring Harb. Symp. Quant. Biol. 27 (1962), 1.
- [13] R.A. Driedonks, Thesis, Leiden (1978).
- [14] F.T. Hesselink, J. Phys. Chem. 73 (1969) 3488.
- [15] C. Tanford, Adv. Protein Chem. 23 (1968) 122.
- [16] H.E. Swaisgood, Crit. Rev. Food Technol. 3 (1972) 375.
- [17] D.G. Schmidt, P. Walstra and W. Buchheim, Neth. Milk Dairy J. 27 (1973) 128.
- [18] C. Holt, A.M. Kimber, B. Brooker and J.H. Prentice, J. Colloid Interface Sci. 65 (1978) 555.